

Evaluation Of Post-Weld Corrosion Behaviour Of Subsea Pipeline In A Marine Environment

Investigation of Angled–Weldment Post-Weld Corrosion Behaviour of Subsea Pipeline in a Marine Environment

Ihom, A.P., Aniekan Offiong, and Obot Patrick Peters

Department of Mechanical Engineering

University of Uyo, PMB 1017, Uyo, Akwa Ibom State, Nigeria

Corresponding Authors email: ihomaondona@uniuyo.edu.ng

Other authors details: irimanagement@yahoo.com, obotuv@yahoo.com or obotman@yahoo.com , 08033973547.

Abstract—This study specifically investigated the influence of groove angles of butt-weld joint of shielded metal arc welding (SMAW) process on the corrosion behaviour of API 5L X-52 linepipe steel in both the natural marine soil and simulated NaCl, Na₂CO₃/NaHCO₃ and Na₂S corrosion environments. Single-V butt-joints of 30°, 45°, 60° and a square butt-joint of 90° were prepared and welded in line with the API 1104 guidelines and details of dimensions for butt-weld joint design using fixed SMAW parameters for investigation. Scanning electron microscope (SEM) and optical emission spectrometer (OES) analyses were performed on the weld bead, HAZ, and base metal of the as-welded X-52 line pipe steel specimens. The study revealed that the amount and nature of heterogeneities that exists among compositions and microstructures of the steel depend on the included groove angle of butt-joint used for joining of the pieces together. The weight loss technique was used to measure the rate of corrosion attack on the as-welded specimens. Sample coupons with known weight were totally embedded in the natural marine soil environment for a total exposure period of 2232 hours, whereas, others were immersed in a non-flowing simulated media of NaCl, Na₂CO₃/NaHCO₃ and Na₂S for a total exposure time of 1008 hours. A total exposure period of 2232 hours was allowed for the marine soil environment before retrieving and reweighing to obtain the final weight of the coupons, while coupon retrieval for the simulated media was carried out every 168 hours for a total period of 1008 hours. The experimental results showed that the corrosion of the X-52 linepipe steel in 2.0 M of NaCl was the highest which was mainly a function of the exposure time and the included groove angles of the butt-weld joint of the samples, followed by 2.0 M solution of Na₂CO₃/NaHCO₃, while the least was recorded for 2.0 M solution of Na₂S. Conclusively it was observed that the corrosion rate of the welded X-52 linepipe steel increased with increase in groove angles of butt-weld joint with the square-butt joint

of 90° being more susceptible to corrosion attack, followed by the 60° and 45° single-V butt joints, while the as-received and as-welded 30° butt weld joint showed least corrosion susceptibility in all the environments.

Keywords—API 5L X52 Linepipe Steel; SMAW; Butt-Weld Joint; Subsea Corrosion Environment; Microstructure

I. INTRODUCTION

Corrosion in oilfield is a major concern, especially when most of the installed infrastructure are aging out with time (Levlin, 1992; Ovri and Ofeke, 1998; Pierre, 2000; Rim-rukeh and Awatefe, 2006). In pipeline construction and installation, welding is needed to join one unit of these pipes to another, and weld corrosion has been identified as a major cause of pipeline failure as most of these pipes are exposed to the atmosphere, buried in soil or marine environment which leads to grievous environmental degradation hence, the need for predicting the integrity of the service life of the pipeline (Santana, Hernandez & Gonzalez, 2003; Beech, 2004; Okoroafor, 2004, Zou, et al., 2005; Zhao, et al., 2007; Ismail and El-Shamy, 2008; Maruthamuthu, et al., 2008; ESAB, 2010). Most common types of corrosion that can occur in a buried pipeline include: (a) pitting corrosion because of material inhomogeneities, (b) chloride or sulphate induced stress corrosion cracking, (c) corrosion by concentration cells in soil arising out of differences in oxygen concentration in the soil adjacent to the pipe at different regions, (d) microbiologically induced/associated corrosion including that caused by sulphate-reducing bacteria (SRB) and acid-producing bacteria (APB), (e) tuberculation because of the build-up of corrosion products on the internal pipe surfaces and, (f) stray current corrosion by earth returns direct currents.

During welding of pipelines heat is transferred to the parent metal, the size of the angle of the joint determines the number of passes of the welding electrode to complete the welding operation. The larger the angle, the more the number of welding passes required and in the process more heat is

introduced into the welded pipe thereby introducing thermal stress in the material upon cooling. This thermal stress remains in the material if heat treatment is not administered after welding operation and has been known to be responsible for stress induced corrosion in the pipeline. The heat from the welding operation as a result of diffusion alters the composition of the parent metal as well as its microstructure stemming from grain recrystallisation, this makes it necessary for homogenizing annealing to be carried out to avoid galvanic corrosion as a result of the presence of anodic and cathodic areas in the welded pipe. The size of the angle of the welded joint is therefore a very important parameter in reducing the amount of heat that goes into the parent metal during welding (Ashby and Easterling, 1982; Fontana, 1986; ESAB, 2010).

Pipelines buried in soil are susceptible to both internal and external corrosions. External corrosion induced by environmental and operational conditions is visible and causes structural deterioration of metallic pipes while internal corrosion remains unnoticeable and ultimately causes significant functional deterioration within distribution system of pipes (Matsushima, 2000; Rajani and Kleiner, 2003). Coating the welded structures with ideal adhesive is frequently used to prevent contact between the linepipe steel and the environment (Santron, 2000). However, degradation of the thus characterized ideal adhesive may contribute to loss of adhesion as it happens frequently when these coatings are exposed to biologically active soil or industrial chemicals exposing the welded pipeline steel structures to prolonged contact with all kinds of natural environments (Jack, Boven, Wilmott and Worthinham, 1996). Protective coatings are subject to abrasion and reapplying of coatings increases the protection cost and traditional coating applications uses toxic volatile organic solvents, causing severe environmental concerns. Hence, in order to solve these problems encountered in present day oilfield and to reduce anticipated ones it is necessary to understand what governs the weldability of these pipes, not least in terms of corrosion failure, from a generic, fundamental metallurgical point of view.

Following from above the objective of this work is to investigate the post-weld behavior of subsea pipeline in a marine environment and simulated environment.

2. MATERIALS AND METHOD

2.1 Materials

The materials used for this study are API 5L X-52 linepipe steel, natural marine soil environment, acetone (degreasing agent), NaCl salt, Na₂S salt, Na₂CO₃ salt, NaHCO₃ salt, E6010 and E7018 Lincoln Electric electrodes. Equipment used included: plastic brush, plastic container, lathe, welding machine, scanning electron microscope equipped with energy dispersive spectroscopy, and electronic digital weighing balance.

2.2 Specimens Preparation

A 4 inches (101.6mm) ID API 5L X-52 grade of steel in form of linepipe with chemical composition as given in Table 1 was obtained from Harmony Steel and Construction Co. Ltd. Port Harcourt. The stock material for the study is available in the required thickness of schedule 80 (8.56mm), outside diameter (OD) of 4.5 inches (114.30mm), and 40 feet (12,192mm) long. The stock X-52 linepipe was cut into 4 inch (101.6mm) length sections by parting process using the turret lathe to obtain the required initial dimensions of the coupon. Fifty-seven (57) pieces of the individual 4 inch sections were further sawed and sheared into 2 inch length and their edges machined with 15°, 22.5° and 30° bevel angles to obtain the required 30°, 45° and 60° groove angles of butt-joints having a root land of 1/16" (1.6mm). A total of nineteen (19) specimens were prepared for each of the studied groove angles of butt-joint. Nineteen (19) pieces of the individual 4 inch sections were also sawed and sheared into 2 inch and their edges prepared as 90° square butt-joint for the study. Dimensional accuracy was tested at random points to ensure material uniformity.

Table 1: Chemical Composition of the Studied API 5L X-52 Steel Pipe

Elements	Weight Percent (%)	Max.
C	0.15562	
Si	0.22471	
Mn	0.96740	
P	0.02571	
Cr	0.03676	
Mo	0.04706	
Ti	0.03067	
Al	0.01233	
Co	0.03567	
V	0.03982	
Fe	98.42425	

2.2.1 Welding Procedure

Single-V butt-joints of 30°, 45° and 60° and a square butt-joint of 90° was prepared and welded in line with the API 1104 guidelines and details of dimensions for butt weld joint design using fixed SMAW parameters. The welding was performed at room temperature and in the 45° inclined welding angle (AWS 6G welding position) with an upward progression of the electrode using the manufacturer's recommended settings for all of the welding parameters and the settings remained consistent while welding the samples.

2.2.2 Microstructure and Composition Test

The three distinct zones (heat affected zone, weld bead and base metal) of the as-welded samples was subjected to microstructure and chemical composition analyses. The PHENOM WORLD – ProX scanning electron microscope equipped with energy dispersive

spectrometer (EDS) and wavelength-dispersive spectrometer (WDS) was used for microstructure analysis and the chemical composition was analyzed using SHIMADZU – PDA: 7000 optical emission spectrometer (OES) equipped with photoelectric photometry. This was done by exposing the well-polished surface of the samples to light emission from the spectrometer. The microstructure, elements contained and their proportions were revealed on the digital processor attached to the spectrometer.

2.3 Corrosion Test

The samples were exposed to a true service corrosion condition generally associated with subsea pipelines with the same atmospheric environment.

2.3.1 Field Exposure Conditions

The marine test site was located 3-5 meters from the Ikot Abasi shore (Imo River) which emptied into the Atlantic Ocean in Akwa Ibom State, Nigeria, at the ALSCON jetty having corrosion parameters as shown in Table 2.

Table 2: Marine Soil Test Site Corrosion Parameters

Soil Parameters

Water Content	65%
pH	5.3
Electrical Conductivity	0.526 ohm-m
Soil Resistivity	1.9 ohm-m
Sulfate Content	1218.88 mg/kg
Iron Content	0.038mg/kg
Potassium Content	205.0 mg/kg
Sodium Content	200.0 mg/kg
Calcium Content	4000 mg/kg
Magnesium Content	780.0 mg/kg
Phosphate	8.80 mg/kg
Population of Sulfide Reducing Bacteria (SRB)	2.0 x 10 ⁵ cfu/ml
Population of Acid Producing Bacteria (APB)	5.00 x 10 ⁵ cfu/ml

2.3.2 Simulated Corrosion Media

Three types of corrosion environments were simulated to determine the weight loss and corrosion rate of the test coupons. Under-listed are the simulated corrosion media:

- i. 2.0 M of NaCl solution (found in marine or seawater)
- ii. 2.0M of Na₂CO₃/NaHCO₃ solution (formed by cathodic over-protection)
- iii. 2.0M of Na₂S solution (contained in the oil and gas fluid)

2.4 Experimental Procedure

The experimental procedure adopted was the total immersion test method in a non-flowing simulated corrosion media because of the good reproducibility of results. Before exposure of the test coupons to the

different corrosion environments, the following steps were adopted.

- i. The samples were cleaned by dipping of the coupons in distilled water for 5 minutes.
- ii. Followed by the use of a soft brush to scrub the specimens.
- iii. Then the coupons were soaked in acetone for 5 minutes before rinsing again.
- iv. They were dried using air blower, and the initial weight (W_1) of the individual coupons using an electronic digital weighing balance was taken.
- v. The dimensions of the samples were then measured to ascertain the exposed surface area of the coupons.
- vi. The weighed coupons were thereafter embedded and immersed in the selected corrosion media for the study.
- vii. After every 7 days (168 hours) of immersion in the simulation media, each of the coupons was brought out and thoroughly cleaned by same procedure as above and weighed again to obtain the final weight (W_2).
- viii. For the marine soil corrosion medium, a total exposure period of 2232 hours (3 months) was allowed before cleaning and reweighing to obtain the final weight (W_2).
- ix. The weight loss (W_f) in milligram and the corrosion rate of the coupons in mm/yr was calculated using the formula below:

$$\text{Weight Loss } (W_f) = W_1 - W_2 \quad (1)$$

Where,

W_f = weight loss in milligrams

W_1 = initial weight of test coupons

W_2 = final weight of test coupons after exposure to soil environment with time

$$\text{Corrosion rate (mm/yr.)} = 87.6 \times W_f / \text{DAT} \quad (2)$$

Where,

W_f = Weight loss in milligrams

D = Density of specimen in g/cm³

A = Total exposed area in cm²

T = Exposure time in hours

$$\text{Exposed Surface Area} = 2\pi rh + 2\pi Rh + 2(\pi R^2 - \pi r^2) \quad (3)$$

Where,

r = internal radius of the pipe in centimetres (cm)

R = external radius of pipe in centimetres (cm)

h = length of the pipe in centimetres
 (cm)
 $\pi = 3.142$

3. RESULTS AND DISCUSSION

3.1 Results

3.1.1 Microstructural Test

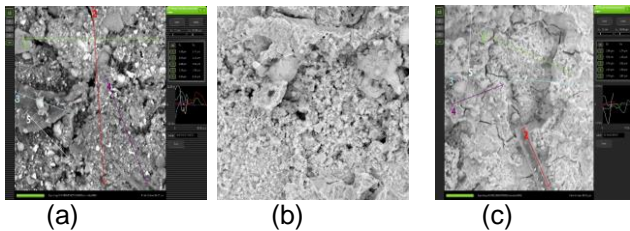


Fig. 1: SEM Micrographs of As-Welded 30° Groove Butt-Joint: (a) Base Metal, (b) HAZ and (c) Weld Bead

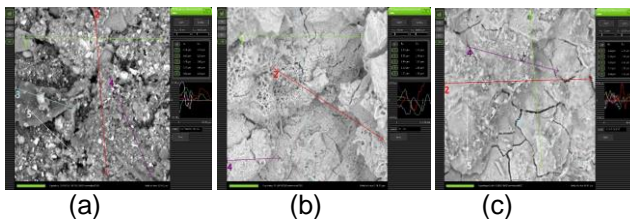


Fig. 2: SEM Micrograph of As-Welded 45° Groove Butt-Joint: (a) Base Metal, (b) HAZ and (c) Weld Bead

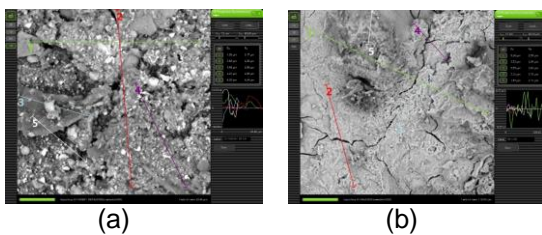


Fig. 3: SEM Micrograph of As-Welded 60° Groove Butt-Joint: (a) Base Metal and (b) HAZ

3.1.2 Compositional Test

Table 3. Chemical Compositions of three Distinct Zones of the As-Welded Butt Joints

Element	Weight Percent (wt. %) Maximum				
		30° Groove		45° Groove	
	BM	HAZ	WB	HAZ	WB
C	0.15562	0.15720	0.21649	0.16247	0.12330
Si	0.22471	0.21841	0.33863	0.21608	0.26444
Mn	0.96740	1.00130	0.58275	0.93263	0.76081
P	0.02571	0.02389	0.02529	0.02677	0.02651
Ni	0.00000	0.00000	0.00000	0.00000	0.00000
Cr	0.03676	0.03936	0.03742	0.04124	0.04559
Mo	0.04706	0.05208	0.05858	0.05657	0.05023
Cu	0.00000	0.00000	0.00000	0.00000	0.00000
Ti	0.03067	0.02932	0.03449	0.02962	0.02202
Pb	0.00000	0.00000	0.00000	0.00000	0.00000
Al	0.01233	0.01426	0.01215	0.01539	0.00934
Co	0.03567	0.04619	0.05434	0.05342	0.05045
W	0.00000	0.00000	0.00000	0.00000	0.00000
V	0.03982	0.04075	0.04379	0.04283	0.04420
Fe	98.45492	98.37724	98.63349	98.43837	98.60311

3.1.3 Weight Loss Test

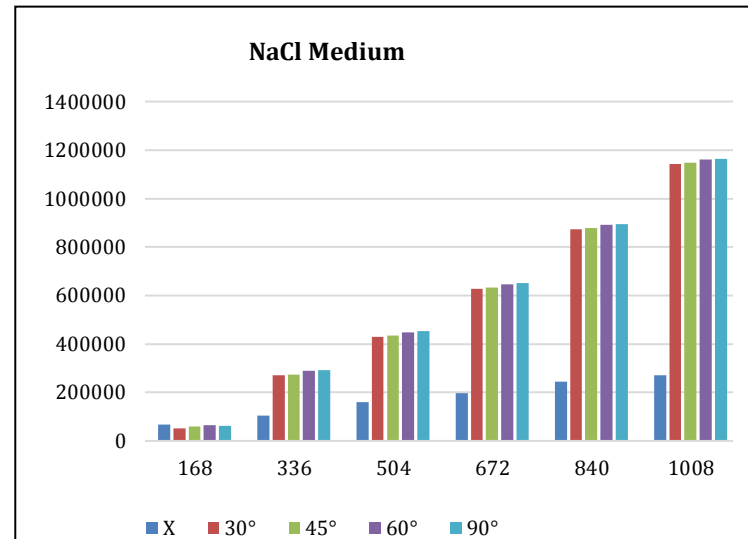


Fig. 4: Weight Loss Recorded for Coupons in 2M NaCl solution

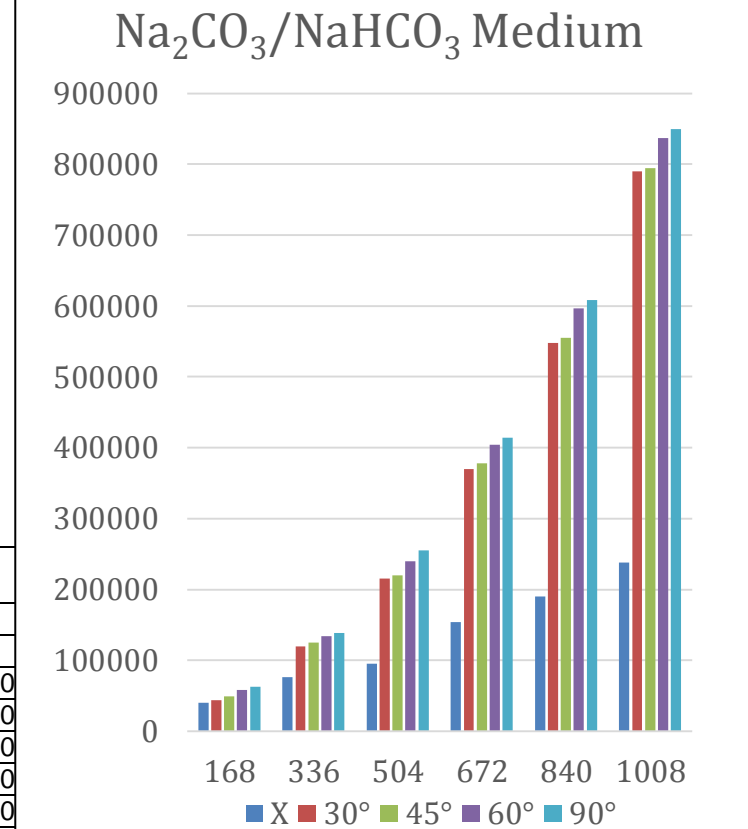


Fig. 5: Weight Loss Recorded for Coupons in 2 M Na₂CO₃/NaHCO₃ Solution

Na₂S Medium

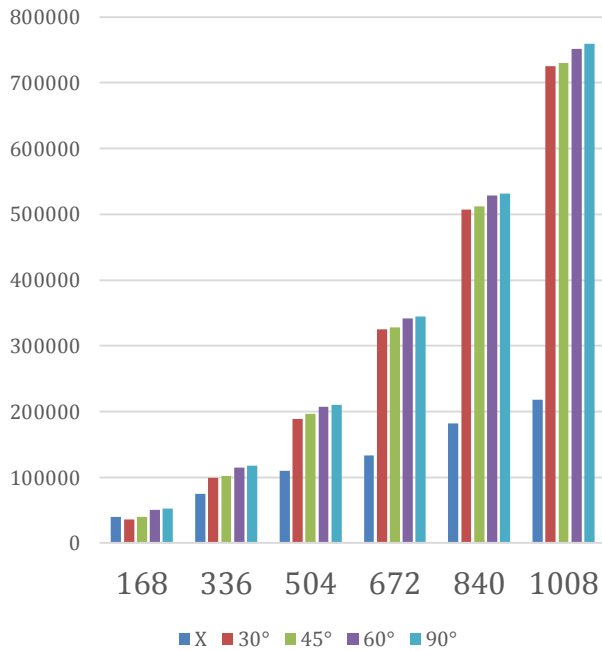


Fig. 6: Weight Loss Recorded for Coupons in 2M Na₂S Solution

Na₂CO₃/NaHCO₃ Medium

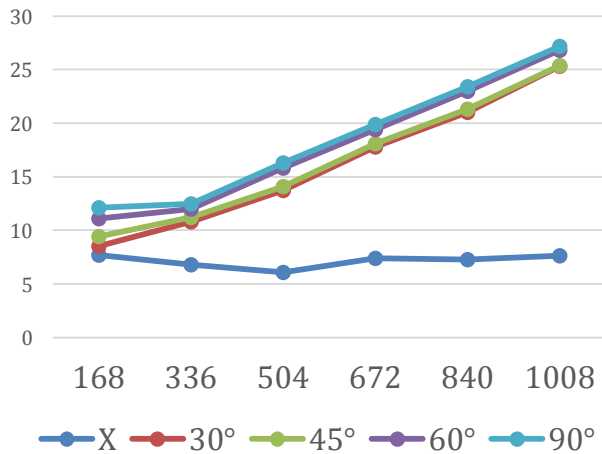


Fig.8: Corrosion Rate Recorded for Coupons in 2M Na₂CO₃/NaHCO₃ Solution

3.1.4 Corrosion Rate Test

NaCl Medium

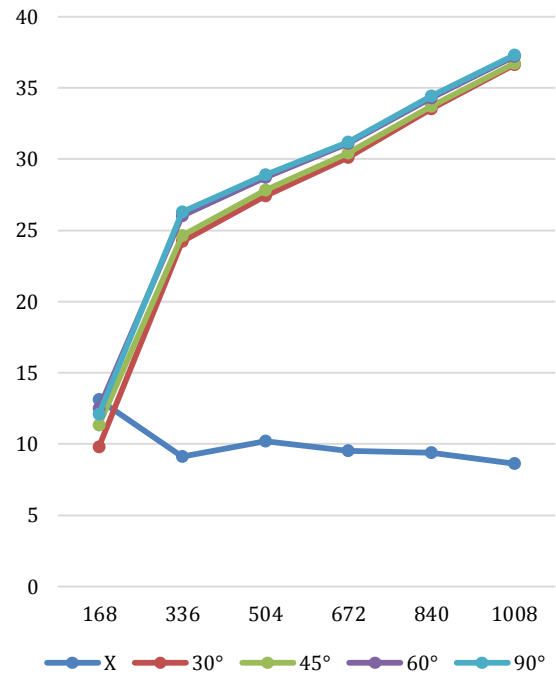


Fig. 7: Corrosion Rate Recorded for Coupons in 2M NaCl Solution

Na₂S Medium

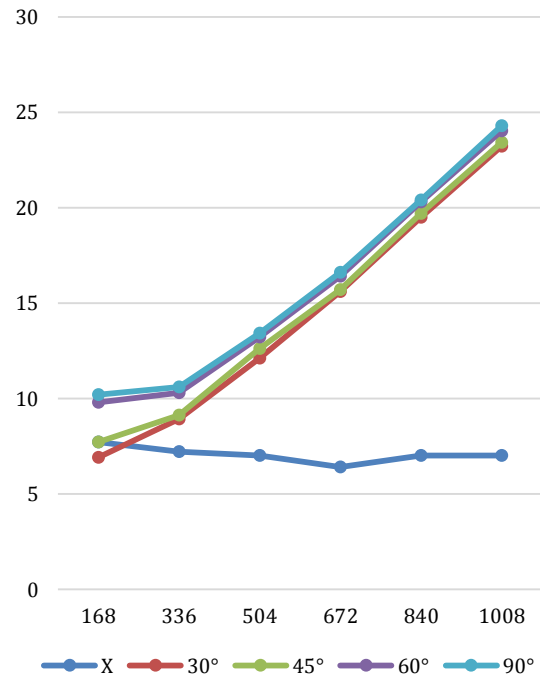


Fig. 9: Corrosion Rate Recorded for Coupons in 2 M Na₂S Solution

3.1.5 Rate of Corrosion Attack on Samples Embedded in Soil

Table 4. Weight Loss and Corrosion Rate of Samples Embedded in Soil

Joint design	Time (hrs)	Initial.wt (kg)	Final wt. (kg)	Wt. loss (mg)	Corrosion rate (mm/yr)
X 93 days	2232	2.138	2.138	-	-
30°	2232	2.222	2.222	-	-
45°	2232	2.260	2.258	2000	0.0289
60°	2232	2.265	2.260	5000	0.0722
90°	2232	2.196	2.191	5000	0.0722

3.2 Discussion of Results

3.2.1 Microstructure Test

Scanning Electron Microscope (SEM) of the as-received X-52 linepipe steel revealed predominantly pearlite phase in a matrix of ferrite with large grains. The dark areas correspond to pearlite and light areas depict the ferrite phase as shown in Figures 1a, 2a and 3a.

Figure 1b shows microstructure of the as-welded 30° butt-weld joint heat affected zone (HAZ), pearlite and ferrite are the two phases present with more volume of ferrite as compared to pearlite. Grain size of the 30° butt-weld joint heat affected zone (HAZ) is seen to be smaller than that of the corresponding base metal (BM).

Figure 1c shows SEM microstructure of the as-welded 30° butt-weld joint weld bead (WB), visibly present are pearlite and ferrite phases with more volume of ferrite as compared to pearlite. Some dark spots are also present while the grain size of 30° butt-weld joint weld bead (WB) microstructure is smaller as compared to both its corresponding base metal (BM) and heat affected zone (HAZ).

The heat-affected zone of the as-welded 45° butt-weld joint sample consists mainly of equiaxed allotriomorphic ferrite which has reformed from the grains and became austenitic and then dynamically recrystallized, Figure 2b.

Figure 2c shows SEM micrograph of the as-welded 45° butt-weld joint, the weld bead has cast structure, which cooled from a temperature above the melting point of the steel. The micrograph depicts a well-defined columnar grains of the microstructure and small equiaxed grains at the centre.

Figure 3b shows microstructure of the as-welded 60° butt-weld joint heat affected zone (HAZ). Here, the parent austenite temperature has cooled from just above A_{c3} which is the correct temperature for annealing resulting in a fine ferrite + pearlite structure.

The micrographs in Figures 1 – 3 depicted a well-defined increase in surface roughness as the included groove angles of butt-joints increases. The highest Rz (mean roughness depth) and Ra (average roughness) occurred on the as-welded 60° butt-joint while the least was noticed on the 30° butt-joint and as-received samples. According to Ashby et al (1982)

the angle of the welded joint determines the number of welding passes to complete the welding processes. As the welding angle increases the number of welding passes also increases. This leads to increase in the heat that enters the welded material thereby increasing the diffusion rate of the elements in the material and bring about compositional changes in the heat affected zone of the welded material (ESAB, 2010). The welded portion itself is like a molten metal solidifying in a cavity so it has a cast structure, typified by cored, columnar and equiaxed (Ashby and Easterling, 1982). The micrographs above agrees with the above explanation as the changes in microstructure can be seen as the welded angles increased.

3.2.2 Chemical Composition Test

Optical emission spectrometer (OES) chemical composition analysis shown in Table 3 revealed the presence of heterogeneities in compositions of the as-welded samples, showing notable changes in the amount of elements present in the weld bead (WB) and heat affected zone (HAZ) when compared to the base metal (BM) of the specimens. The changes are a function of weld thermal cycle of heating and cooling which occur during the SMAW process brought about by diffusion. The as-welded 90° square butt-joint samples showed the highest variation in chemical composition of the weld bead and adjacent base metal. Ashby and Easterling (1982) said as the welded angle increases diffusion rate increases this brings about chemical compositional change in the material. This can be seen in Table 3.

3.2.3 Weight Loss Test

Figure 4 shows plot of samples cumulative weight loss against time of exposure in 2.0 M concentration of sodium chloride (NaCl) solution. It is observed that the samples loss weight with increasing exposure time; trend of weight loss is in increasing order of 30° square butt-joint, 45°, 60°, and 90° single-V butt-joints, while the un-welded samples showed least weight loss.

Figure 5 is a plot of cumulative weight loss of the samples against exposure time in 2.0 M concentration of sodium carbonate/sodium bicarbonate ($Na_2CO_3/NaHCO_3$) solution. The 30° and 45° single-V butt-joints was seen to lose weight at almost the same rate, and the 90° square butt-joint and 60° single-V butt-joint was also observed to have lost weight at almost the same rate. From the plot in Figure 5, there occur a significant rate of weight loss for the as-welded 30°, 45° and 60° single-V butt-joints and 90° square butt-joint samples as compared to that of the samples not welded. A relatively significant difference in rate of weight loss is observed.

Figure 6 shows weight loss characteristics of the samples over exposure time in a solution containing 2.0 M concentration of sodium sulfide (Na_2S). The as-received and the 45° single-V butt-joint samples was found to exhibit an initial same rate of weight loss while the 30° single-V butt-joint was observed to have had the lowest initial weight loss. On

further exposure to the environment, a rather high weight loss was observed and between exposure time range of 336 hours and 1008 hours, the as-welded 30°, 45° and 60° single-V butt-joints showed sharp increase in weight loss with the as-received samples showing gradual increase in weight loss value, while the 90° square butt-joint samples revealed the highest weight loss value. It has been observed by several researchers that welding introduces thermal stresses to the welded material and to relief these stress heat treatment is required. Ashby et al have equally observed that thermal stresses increases with welding passes it is therefore not surprising that the weight loss is highest with the 90° weld joint the biggest angle is expected to have the highest thermal stress since the specimens were not heat treated. Thermal stress induces stress corrosion and this form of corrosion is very common with welded materials.

3.2.4 Corrosion Rate Test

Figure 7 shows cumulative corrosion rate characteristics of the samples over exposure time in a solution containing 2.0 M sodium chloride (NaCl) solution. The 30°, 45° and 60° single-V butt-joints samples and the 90° square butt-joint samples were found to exhibit lower initial corrosion rate values as compared to that of the as-received samples which showed high initial corrosion rate value. On further exposure to the environment, increase in corrosion rate value of the welded samples were observed, and between exposure time range of 336 hours and 1008 hours, the welded 30°, 45° and 60° single-V butt-joints samples showed gradual increase in corrosion rate, while the 90° square butt-joint samples revealed the highest corrosion rate value. Between exposure time range of 504 hours and 1008 hours, the as-received samples showed gradual decrease in corrosion rate value.

Cumulative corrosion rate characteristics of the samples in 2.0M sodium carbonate/sodium bicarbonate ($\text{Na}_2\text{CO}_3/\text{NaHCO}_3$) solution over exposure time is shown in Figure 8. For the welded 30°, 45° and 60° single-V butt-joints and 90° square butt-joint samples, an initial gradual increase in corrosion rate occurred between 168 hours and 336 hours of exposure time. Subsequently, a sharp increase in corrosion rate up to 1008 hours was noticed, the welded 30° single-V butt-joint samples showed less initial to final corrosion rate values as compared to that of the welded 45°, 60° and 90° butt-joint samples, with increasing time of exposure, the 90° square butt-joint samples was found to lose weight more rapidly relative to the welded 30° and 45° single-V butt-joints samples. The as-received samples showed an initial decrease in corrosion rate between 168 hours and 504 hours and a final increase in corrosion rate between 672 hours and 1008 hours of exposure time.

Figure 9 shows cumulative corrosion rate characteristic of the samples over exposure time in a solution containing 2.0 M sodium sulfide (Na_2S) solution. The as-received samples was found to exhibit an initial gradual decrease in corrosion rate. On further exposure to the environment, a rather

constant corrosion rate between exposure time range of 840 hours and 1008 hours was observed. And between exposure time range of 168 hours and 1008 hours, the as-welded 30°, 45° and 60° single-V butt-joint samples showed gradual increase in corrosion rate, while the 90° square butt-joint samples revealed the highest corrosion rate value.

From Figures (7 – 9) it is clear that the speed or rate of deterioration of the subsea transmission pipelines for oil and gas will depend on the environmental conditions and the type and condition of the metal under reference. This dissimilar-metal couple produces macroscopic galvanic corrosion and influences the corrosion process in the vicinity of the weld. It has been observed by several researchers that welding introduces thermal stresses to the welded material and to relief these stress heat treatment is required. Ashby and Easterling (1982) have equally observed that thermal stresses increases with welding passes it is therefore not surprising that the weight loss is highest with the 90° weld joint the biggest angle is expected to have the highest thermal stress since the specimens were not heat treated. Thermal stress induces stress corrosion and this form of corrosion is very common with welded materials (Fontana, 1986).

3.2.5 Rate of Corrosion Attack on Samples Embedded in Soil

Table 4 shows weight loss and corrosion rate of the samples, as well as exposure time of the samples embedded in the natural marine soil environment. The as-received and welded 30° single-V butt-joint samples was seen to exhibit excellent passive corrosion behaviour in the studied environment while active corrosion behaviour was more pronounced in the welded 90° and 60° butt-joint samples. The 90° square butt-joint and 60° single-V butt-joint was observed to have lost weight at the same rate. From Table 4, there occur a significant rate of weight loss for the welded 60° single-V butt-joint and 90° square butt-joint samples as compared to that of the 45° and 30° single-V butt-joints and the as-received samples. 'X' represent the as-received X-52 linepipe steel used as control coupons for the experiment.

The slow rate of corrosion behaviour of the X-52 linepipe steel exposed to the natural marine soil environment, as shown in Table 4, is due to its high corrosion resistance and the ability of the material to develop passivity to the environment. Other reasons include the following: low conductivity of the soil, low sulfide reducing bacteria (SRB), low concentration of aggressive ions such as chlorides and sulphates as can be seen in Table 2 (Fontana, 1986).

4. CONCLUSION

The study on evaluation of post-weld corrosion behaviour of subsea pipelines in a marine environment conducted by weight loss and corrosion rate measurements has been successfully carried out and the following conclusions drawn:

- i. Welding introduces thermal stresses and compositional changes into welded

- materials which increase as the weld passes increases as a result of increase in weld angle.
- ii. The weld-bead or weldment has the microstructure of a solidified casting, typified by cored, columnar and equiaxed structures.
 - iii. The heat affected zone (HAZ) chemical composition and microstructure is determined by the number of welding passes which in turn depends on the included angle of butt-welded joint in the absence of heat treatment.
 - iv. The corrosion rate of the steel coupons depend on the included groove angle of butt-weld joint used, thermal stress, compositional and microstructural changes.
 - v. The low corrosion rate of the as received specimens in marine soil environment and simulated environment is attributed to the specimens high corrosion resistance and its ability to develop passivity.

REFERENCES

- Ashby, M.F. and Easterling, K.E. (1982) A 1st Report on Diagrams for Grain-growth in Welds Acta Metallurgica. Inc. vol.30, pp1969-1978
- Beech, I. B. and Sunner, J. (2004). Bio-corrosion: Towards Understanding Interaction between Biofilms and Metals. *Current Opinion in Biotechnology, Elsevier*, Vol. 15, pp. 181 – 186.
- ESAB Aberdeen, (2010). Welding Techniques, Welding Consumables, Defects and Remedies, Sweden. Aberdeen: *Pipelines Welding Handbook*, ESAB AB, pp. 4 – 18.
- Fontana, M.G. (1986) Corrosion Engineering, 3rd Edition, USA: Mcgraw Hill Book Company, USA.
- Ismail, A. I. and El-Shamy, A. M. (2008). Engineering Behaviour of Soil Materials on the Corrosion of Mild Steel. *Applied Clay Science*, No. 30, pp. 42 – 45.
- Jack, T. R., Boven, G., Wilmott, M. and Worthinham, R. G. (1996). Evaluating Performance of Coatings Exposed to Biologically Active Soils. *Material Performance*, No. 35, pp. 39 – 45.
- Levlin, E. (1992). Corrosion of Water Pipe Systems due to Acidification of Soil and Groundwater. Department of Applied Electro-chemistry and Corrosion Science, Royal Institute of Technology, Stockholm. Sweden.
- Maruthamuthu, S., Muthukumar, M., Natesan, N. and Palaniswamy, N. (2008). Rule of Air Microbes on Atmospheric Corrosion. *Current Science*, Bangalore, India, Vol. 94(3), pp. 359 – 363.
- Matsushima, I. (2000). Carbon Steel-Corrosion by Soil. Uhlig's Corrosion Handbook, 2nd ed., USA: *John Wiley & Sons, Inc.*, pp. 329 – 348.
- Okoroafor, C. (2004). Cathodic Protection as Means of Saving National Asset. *Journal of Corrosion Science and Technology*, Special Edition, pp. 1 – 6.
- Ovri, J. E. and Ofeke, T. B. (1998). The Corrosion Behaviour of Mild Steel in Marine Environment. *Journal of Science, Engineering and Technology*, Vol. 5(2), pp. 1117 – 1129.
- Pierre, R. R. (2000). Handbook of Corrosion Engineering. USA: *McGraw-Hill*, New York, ISBN 0-07-076516-2 2000, p. 142.
- Pope, D. and Morris, E. (1995). Mechanisms of Microbiologically Induced Corrosion (MIC). *Materials Performance*, Vol. 34(5), pp. 24.
- Rajani, B. and Kleiner, Y. (2003). Protection of Ductile Iron Water Mains against External Corrosion: Reviews of Methods and Case Histories. *Journal of American Water Works*, No. 95, pp. 110 – 125.
- Rim-rukeh, A. and Awatefe, J. K. (2006). Investigation of Soil Corrosivity in the Corrosion of Low Carbon Steel Pipe in Soil. *Journal of Applied Sciences Research*, New York, USA, Vol. 2(8), pp. 466 – 469.
- Santana, J. J., Hernandez, F. J. and Gonazalez, J. E. (2003). The Effect of Environmental and Meteorological Variables on Atmospheric Corrosion of Carbon Steel, Copper, Zinc and Aluminum in a Limited Geographic zone with Different Types of Environment. *Corrosion Science*, Bangalore, India, Vol. 45, pp. 799 – 815.
- Santron, J. B. (2000). Paint and Coating: New Trend Respond to Environmental Concerns. *Material Performance*, No. 39, pp. 22 – 25.
- Srikanth, S., Sankaranarayanan, T. S., Gopalakrishna, K., Narasimhan, B. R., Das, T. V. and Das, S. W (2005). Corrosion in a Buried Pressurized Water Pipeline. *Engineering Failure Analysis*, Vol. 12(4), pp. 634 – 651.
- Zhao, X., Duan, J., Hou, B. and Wu, S. (2007). Effect of Sulphate-Reducing Bacteria on Corrosion Behaviour of Mild Steel in Sea Mud. *Journal of Materials Science and Technology*, Shenyang, China, Vol. 23(3), pp. 323 – 328.
- Zou, R., Kus, E., Mansfeld, F. and Wood, T. K. (2005). The Importance of Live Biofilms in Corrosion Protection. *Corrosion Science*, Vol. 47, pp. 279 – 287.